ACS Sustainable Chemistry & Engineering

pubs.acs.org/journal/ascecg

Research Article

Selective CO_2/CH_4 Separation by Fixed-Bed Technology Using Encapsulated Ionic Liquids

J. Lemus,* C. Paramio, D. Hospital-Benito, C. Moya, R. Santiago, and J. Palomar

Cite This: *ACS Sustainable Chem. Eng.* 2022, 10, 13917−13926

Read Online

ACCESS | Metrics & More | Article Recommendations | Supporting Information

ABSTRACT: The performance of encapsulated ionic liquid (ENIL) sorbents has been experimentally evaluated in CO_2/CH_4 separation by means of gravimetric and fixed-bed measurements. Six ionic liquids (ILs) with CO_2 chemical absorption ([Emim][Acetate], [Bmim][Acetate], [P_{66614}][CNPyr], [Bmim][GLY], [Bmim][MET], and [Bmim][PRO]) were selected for the selective separation of CO_2 from CH_4. ENIL materials were prepared by encapsulation of these ILs in synthesized carbon submicrocapsules, achieving a ∼70% in mass of IL. Fixed-bed experiments of CO_2 capture were carried out to evaluate the CO_2/CH_4 separation performance of prepared ENIL materials at different CO_2 partial pressures and 303 K. Both thermodynamics and kinetics of CO_2 sorption were analyzed. The experimental CO_2 and CH_4 isotherms in ENIL materials obtained from fixed-bed experiments were successfully compared to those obtained by reliable gravimetric tests and fitted to the Langmuir−Freundlich equilibrium model. In addition, experimental CO_2 breakthrough curves were well-described by the linear driving force and Yoon and Nelson kinetic models, providing sorption rate constants. ENIL sorbents show high CO_2 uptake capacity, comparable to conventional adsorbents, but with drastically higher selectivity, in concordance with the negligible CH_4 solubility in ILs at the used operating conditions, with acetate-based ENIL materials being the best sorbents in thermodynamic terms. The obtained kinetic parameters revealed that the CO_2 chemical sorption with ENIL materials overcomes the IL mass transfer limitations. The sorption rates are faster than those obtained with ENIL using IL physical absorbents and seem to be controlled by the reaction kinetics. The [P_{66614}][CNPyrr]-based ENIL is found to be the most promising material, combining favorable kinetic and thermodynamic considerations for future development of CO_2/CH_4 separation using fixed-bed technology.

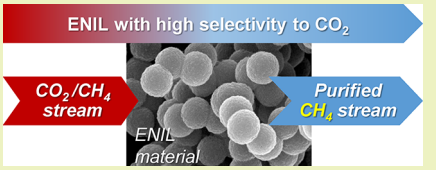

KEYWORDS: *CO_2 capture, CO_2/CH_4 separation, encapsulated ionic liquid, carbon capsule, fixed-bed*

INTRODUCTION

Carbon dioxide (CO_2) capture is a beneficial technology for the worldwide decarbonization due to its effectiveness and relatively low cost.[1,2] CO_2 capture technology is broadly used to remove CO_2 compounds from industrial plants.[3,4] Nowadays, the CO_2 separation from natural gas and biogas streams to enhance the quality of the methane (CH_4) product[5,6] is essential to guarantee its safety, transportation, and growing utilization.[7−9] In this respect, numerous CO_2 capture approaches have been proposed.[10] Technologies based on amine scrubbing work effectively for CO_2 chemical capture through the formation of organic compounds, as carbamate and carbonate,[11,12] but they can cause serious solvent losses, corrosion problems, and a regeneration stage with a high energy demand.[13] In this sense, a promising alternative thoroughly investigated is ionic liquids (ILs), using them as potential CO_2 absorbents since they present favorable properties like high uptake capacity, negligible vapor pressure, wide liquid temperature range, and tunable solvent behavior.[14,15] Two alternative types of ILs attending to the CO_2 absorption are being studied.[16] ILs with CO_2 physical absorption require high operating pressures to obtain a competitive CO_2 solubility.[17] Nevertheless, ILs with chemical absorption of CO_2[18] seem to be the most convenient approach for CO_2 retention, with acetate-based ILs,[19−21] aprotic heterocyclic anion-based ILs (AHA-ILs),[22−24] or amino acid-based ILs (aa-ILs)[25−27] being the most promising alternatives.[28,29] Although ILs present a significant impact on CO_2 capture due to their unique characteristics, their mass transport properties are still a main constraint for practical applications.[16,30] ILs with chemical CO_2 absorption exhibit a much higher viscosity than conventional amine solutions used for CO_2 capture. In recent works, the mass transport limitation of ILs has been overcome by increasing the gas−liquid contact surface through solvent encapsulation in micro or submicroparticles.[17,31,32] Encapsulated ionic liquids (ENIL) prepared with porous carbon capsules allowed introducing a huge amount of ILs inside them (until 80 wt %).[33] This high amount of ILs makes ENIL suitable to achieve a high CO_2 uptake, with the CO_2 chemical sorption rate being simultaneously drastically increased.[21,24,27] Thus, it has been

Received: April 27, 2022
Revised: September 2, 2022
Published: October 12, 2022

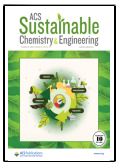

demonstrated that ENIL evades the kinetic limitations of neat ILs, and the CO_2 physical capture efficiency in fixed-bed technology is determined by the thermodynamics of the mixture, in contrast with the packed column absorption using ILs, which is controlled by kinetics.[17] Moreover, CO_2 chemical absorption with ILs lets an efficient solvent use[27] and regeneration[21] thanks to the IL encapsulation. On the other hand, it was recently demonstrated that CO_2 capture in fixed-bed technology with supported ILs (SILP) shows that the sorption rate is controlled by the chemical reaction (CO_2-IL) for particle sizes below 0.15 mm.[34] In this sense, as ENIL presents a smaller diameter (~0.8 μm) than SILP, an efficient use is expected in the CO_2 chemical capture process using a fixed bed. Additionally, a recent work by Durak *et al.*[9] demonstrated growing enhancement in CO_2/CH_4 selectivity of an ordinary activated carbon by supporting increasing amounts of acetated-based ILs from 5 to 35 wt %. As the ENIL sorbent is incorporated until 80 wt % of the IL, high performance is expected for CO_2/CH_4 gas separation in a fixed bed using the ENIL sorbent.

Therefore, the main objective of the present study is the detailed analysis, considering both thermodynamic and kinetic aspects, of six different ILs with CO_2 chemical absorption in their development as ENIL materials in the selective CO_2/CH_4 separation by fixed-bed processes. The treatment of CO_2/CH_4 streams with ENIL for selective separation is studied for the first time in the present work. ILs used to prepare ENIL materials were carefully selected attending to previous evidence of their performance in CO_2 capture. All of them present a reversible reaction with CO_2 and high absorption capacity. The amino acid-based ILs (1-butyl-3-methylimidazolium prolinate, [Bmim][PRO]; 1-butyl-3-methylimidazolium methioninate, [Bmim][MET]; and 1-butyl-3-methylimidazolium glycinate, [Bmim][GLY]) were selected because they are environmentally better candidates and the ENIL procedure avoids the kinetic problems, making them promising materials.[27,35] The acetate-based (1-ethyl-3methylimidazolium acetate [Emim][Acetate] and 1-butyl-3-methylimidazolium acetate [Bmim][Acetate])[21] and aprotic heterocyclic anion-based (trihexyltetradecylphosphonium 2-cyanopyrrolide [P_{66614}][CNPyrr])[24] ILs were tested to capture CO_2 from CH_4-rich streams because they were reported solvents with excellent process performance in chemical CO_2 absorption for biogas purification,[28,29] whose sorption−desorption rates were significantly increased by ENIL systems.[21,24] Prepared and characterized ENIL materials were evaluated in fixed-bed experiments feeding a $CO_2/CH_4/N_2$ gas mixture at 303 K and CO_2 partial pressures from 0.04 to 0.4 bar, by measuring the breakthrough curves of the mixture compounds, which were complemented with CO_2 and CH_4 isotherms obtained by gravimetric measurements. Thermodynamic and kinetic parameters have been evaluated in order to assess ENIL sorbent materials in the CO_2 capture process. The models used to fit the experimental breakthrough curves were the Yoon and Nelson model and the linear driving force model with a lumped resistance, which let us to estimate the corresponding sorption rate constants, whereas obtained equilibrium isotherms were adjusted with the Langmuir−Freundlich model. These mathematical models let us to evaluate the performance of ENIL materials tested in CO_2/CH_4 separation by fixed-bed technology.

EXPERIMENTAL SECTION

Materials. The ILs used in this study were two acetate-based ILs (1-ethyl-3methylimidazolium acetate [Emim][Acetate] and 1-butyl-3-methylimidazolium acetate [Bmim][Acetate], supplied by Sigma-Aldrich at >95% purity), an aprotic heterocyclic anion-based IL, [P_{66614}][CNPyrr], synthesized and purified in our laboratory as previously detailed,[24] and three amino acid-based ILs, 1-butyl-3-methylimidazolium prolinate [Bmim][PRO], 1-butyl-3-methylimidazolium methioninate [Bmim][MET], and 1-butyl-3-methylimidazolium glycinate [Bmim][GLY] supplied by Iolitec at >95% purity. Both [Bmim][PRO] and [Bmim][MET] were used as a racemic mixture.

ENIL Preparation and Characterization. The first step for the ENIL preparation was the synthesis of carbon capsules (C_{cap}) used as a support of the ILs. This procedure was a replication of our methodology reported in previous works.[33,36] Summarizing, C_{cap} were obtained following the Stöber synthesis,[37] by a templating method using a solid core−mesoporous shell aluminosilicate template. A phenolic resin was infiltrated into the template to serve as a carbon precursor. Then, the infiltrated template was subjected to pyrolysis at 973 K for 5 h under a N_2 atmosphere. The resulting carbon aluminosilicate was washed with HF (48%) to generate hollow core−mesoporous shell carbon. These C_{cap} were filled with ILs by means of direct impregnation, solving the amount required of ILs in acetone.[38] To prevent hydration, ILs and acetone were kept in their original tightly closed bottles in a desiccator before use. Impregnation was carried out by mixing 1 mL of ILs dissolved in acetone for each 100 mg of C_{cap}. To ensure a homogeneous penetration of the IL solution into the pores, the IL solution was added drop by drop over the surface of the C_{cap}. Then, synthesized ENIL materials were stored at 333 K for 24 h prior to their use. In the current work, the six ENIL tested were prepared with an IL nominal load of 65−75 wt %, using elemental analysis to quantify the amount of IL incorporated into the capsules.[35,38]

In terms of material characterization, the morphology of C_{cap} used as a support was studied by scanning and transmission electron microscopy (SEM and TEM). SEM micrographs were obtained using a Hitachi S-3000N model microscope and TEM images in a JEOL JEM 2100 HT microscope. Then, the porous structure was characterized by means of N_2 adsorption−desorption isotherms at 77 K on a Micromeritics apparatus (Tristar II 3020 model). The samples were previously outgassed at 333 K, and a vacuum of 0.01 bar was applied for 6 h. The thermal stability of ENIL materials was evaluated by thermogravimetric analysis (TGA) using a DSC/DTA/TGA module from TA Instruments under a N_2 atmosphere within the range of 298−923 K with a heat rate of 5 K/min. The masses of the samples placed in TGA analyses were between 5 and 10 mg using alumina pans with a capacity of 70 mL. The accuracy of temperature was 0.1 K, and that of mass measurements was 10^{-3} mg. Additionally, elemental analyses (EA) of ENIL materials were conducted with a PerkinElmer analyzer (210 CHN model) to obtain C, H, and N contents.

CO_2/CH_4 Fixed-Bed Capture Experiments. The fixed-bed experiments were carried out in a Microactivity unit (PID Eng&Tech, Spain) provided with a vertical quartz tube of 1.6 cm internal diameter and 20 cm length. The tube was placed into a furnace to control the temperature from room temperature to 573 K. The pressure inside the fixed bed can be controlled from atmospheric to 20 bar. The outlet gas flow was analyzed by an Agilent 7820A gas chromatograph equipped with a 20 m column (Agilent PoraPlot U) and a thermal conductivity detector (TCD) and a flame ionization detector (FID), which allowed us to calculate the CO_2 and CH_4 concentrations, respectively. For each experiment, the fixed bed was loaded with ~2−4 g of fresh ENIL, i.e., a bed height between 3.5 and 5.7 cm. The inlet gas, composed of a CO_2/CH_4 mixture (40/60 v/v of CO_2/CH_4) or in dilution with N_2, was continuously fed through the fixed bed with a constant flow of 16 NmL/min, trying six different CO_2 partial pressures (0.4, 0.32, 0.24, 0.16, 0.08, and 0.04 bar). Therefore, for each ENIL tested, six breakthrough curves at 303 K, maintaining a 1 bar total pressure, were obtained. The pressure was

https://doi.org/10.1021/acssuschemeng.2c02504
ACS Sustainable Chem. Eng. 2022, 10, 13917−13926

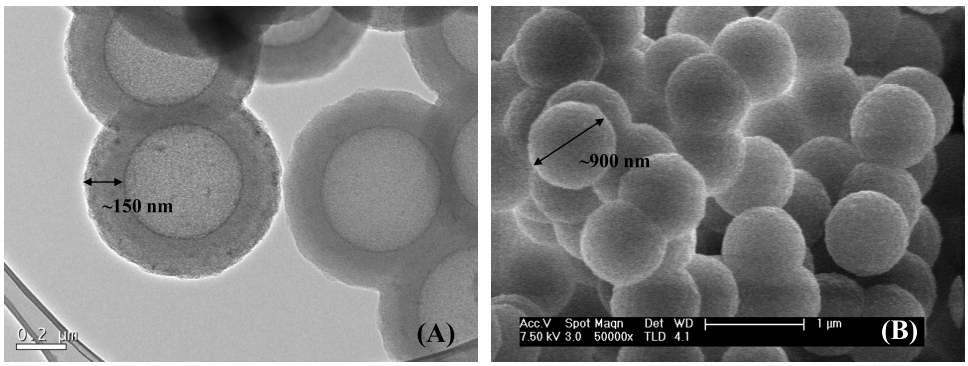

Figure 1. (A) TEM and (B) SEM images of C_{cap}.

measured before the fixed-bed column, and the outlet pressure was atmospheric. The entry pressure at any moment was over 0.1 bar (instrument precision); it means that the pressure drop was under 0.1 bar.

Once the ENIL material was saturated, the furnace temperature was increased to 333 K for its regeneration. We did not notice any difference in capacity before and after the regeneration step, which allowed us to use the ENIL material in different sorption−desorption cycles. A blank experiment was performed with the fixed-bed column loaded with inert material (glass beads) covering the same bed height as the ENIL. In that way, the calculations were done by subtracting the blank measurement curve at each temperature from the breakthrough curve of each ENIL material at that temperature. The mass sorption capacity (q_e, g/kg_{ENIL}) was calculated from the breakthrough curves using the following equation:

$$q_e = \frac{Q}{m_{ENIL}} \cdot \int_0^{t_s} (C_0 - C)\, dt \tag{1}$$

where Q is the gas flow rate (L/min), m_{ENIL} is the ENIL mass (kg) in the fixed bed, C and C_0 are respectively the outlet and gas inlet concentrations (g/L), and t_s is the saturation time (min). For comparison purposes, the molar sorption capacities of ENIL (W_{CO_2}, mol_{CO_2}/kg_{ENIL}) and ILs (W_{CO_2}, mol_{CO_2}/kg_{IL}) were also estimated by considering the CO_2 molar weight and the amount of ILs incorporated in ENIL materials, to obtain the sorption isotherm at the studied CO_2 partial pressure range.

Gravimetric CO_2 Sorption Experiments. Measurements of the CO_2 sorption capacity of ENIL material (W_{CO_2}, mol_{CO_2}/kg_{ENIL}) were also performed in a gravimetric high-pressure sorption analyzer (IsoSORP gas LP-flow, Rubotherm) equipped with a magnetic suspension balance (MSB). The microbalance included a weight range up to 10 g with a precision of 10^{-5} g. The CO_2 sorption isotherms for the six ENIL materials were obtained at 303 K and a pressure range from 0.3 to 20 bar. In a typical run, a 100 mL/min flow of pure CO_2 (also pure CH_4, isotherms in the Supporting Information) at 1 bar was passed through the sorbent sample (~100 mg of ENIL materials), and the mass increase was recorded over time at a fixed temperature. Once the sample was saturated, i.e., the weight change was <0.02 mg/h, the pressure was increased. Lastly, the amount of CO_2 (or CH_4) absorbed was quantified, previously correcting the buoyancy effect, as it was reported in previous works.[34]

Thermodynamic and Kinetic Models. *Isotherm Modeling.* Experimental CO_2 isotherms were modeled by using the available estimation module implemented in Aspen Adsorption v10.0 software. The Langmuir−Freundlich model is shown in eq 2. The gases used (CO_2, CH_4, and N_2) were selected from the Aspen Properties database, choosing Peng−Robinson as the equation of state. It was confirmed that CH_4 and N_2 present a negligible sorption in our materials.[14]

$$W_{CO_2}\left[\frac{mol}{kg_{ENIL}}\right] = \frac{IP_1 \cdot IP_2 \cdot p_{CO_2}^{IP_3} \cdot e^{IP_4/T}}{1 + IP_5 \cdot p_{CO_2}^{IP_3} \cdot e^{IP_6/T}} \tag{2}$$

where W_{CO_2} is the equilibrium CO_2 sorption capacity at each partial pressure; p_{CO_2} is the CO_2 partial pressure (bar); T is the temperature (K), and IP_1, IP_2, IP_3, IP_4, IP_5, and IP_6 are the fitting parameters of the equation.

Breakthrough Curve Modeling. The breakthrough curves were fitted to the equation described by Yoon and Nelson:[39]

$$t = t_{0.5} + \frac{1}{k_{YN}} \cdot \ln\left(\frac{C}{C_0 - C}\right) \tag{3}$$

where t is the operation time (min), $t_{0.5}$ is the time when the outlet concentration is half of the inlet one (min), C and C_0 are respectively the outlet and inlet CO_2 gas concentrations (g/L), and k_{YN} is the Yoon and Nelson constant (min^{-1}), which is used in our study as the effective rate constant for comparing the used ENIL materials, defined as follows:

$$k_{YN}\ (min^{-1}) = \frac{k \cdot C \cdot Q}{q_e} \tag{4}$$

where k is a proportionality constant (kg_{ENIL}^{-1}), C is the inlet CO_2 concentration (g/L), Q is the gas flow rate (L/min), and q_e is the CO_2 mass capacity (g/kg_{ENIL}). This model has been successfully applied in fixed-bed sorption operations using conventional solid adsorbents[39−41] and encapsulated ILs.[17] The length of the mass transfer zone (H_{MTZ}) was calculated from each breakthrough curve as an additional parameter to evaluate the kinetics of the process using the following equation:

$$H_{MTZ} = H \cdot \frac{(t_{0.95} - t_{0.05})}{t_{0.95}} \tag{5}$$

where H is the height of the bed and $t_{0.05}$ and $t_{0.95}$ are the times at which the outlet CO_2 concentration reaches 5 and 95% of the inlet one, respectively.

Alternatively, the pseudo-first-order linear driving force (LDF) kinetic model has been implemented to describe mass transfer between the gas and the ENIL sorbent since it was previously applied to analyze the CO_2 capture in a fixed bed using supported ILs.[34] Aspen Adsorption software was used to fit experimental breakthrough curves, by means of the kinetic model named LDF:

$$\frac{\partial W_{CO_2}}{\partial t} = k_{MTC} \cdot (W_{CO_2}{}^{*} - W_{CO_2}) \tag{6}$$

It considers all resistances to mass transfer lumped as a single overall factor or a resistance that controls mass transfer. The driving force is a function of CO_2 mass sorbent capacity. The values of the effective kinetic coefficient (k_{MTC}) were calculated by fitting the measured data of breakthrough curves in fixed-bed experiments. To

https://doi.org/10.1021/acssuschemeng.2c02504
ACS Sustainable Chem. Eng. 2022, 10, 13917−13926

Table 1. IL Structures, Properties at 298 K, and ENIL Characterization

	IL structure		MW_{IL}	ρ_{IL}	μ_{IL}	%IL	%IL
	Cation	anion	(g/mol)	(g/cm^3)	(mPa/s)	EA	TGA
[Emim][Acetate] [43]			170	1.09	133	65	63
[Bmim][Acetate][21]			198	1.03	180	68	66
[P_{66614}][CNPyr] [24]			574	0.90	166	68	68
[Bmim][GLY] [27]			213	1.06	550 (313 K)	59	59
[Bmim][PRO][27]			253	1.08	891 (313 K)	75	71
[Bmim][MET] [27]	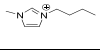		287	1.10	660 (313 K)	68	68

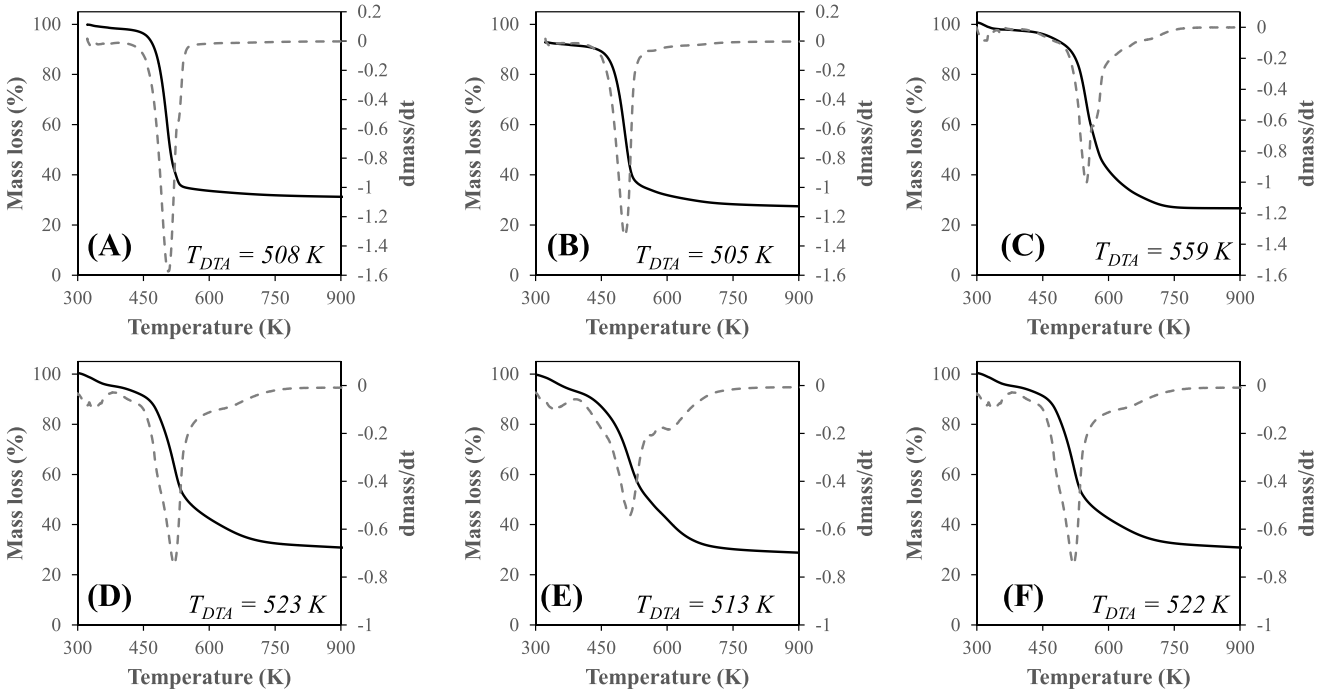

Figure 2. TGA of ENIL (black solid line) and DTA (gray dashed line) curves of (A) [Emim][Acetate], (B) [Bmim][Acetate], (C) [P_{66614}][CNPyr], (D) [Bmim][GLY], (E) [Bmim][MET], and (F) [Bmim][PRO] under a nitrogen atmosphere with a heating rate of 5 K/min.

achieve this, some bed parameters and the operating conditions must be entered into the simulator as input information (bed size, particle radius, bed and particle porosity, bulk sorbent density, and operating conditions as pressure, temperature, inlet molar flow, and inlet CO_2 partial pressure, see details in Table S1 of the Supporting Information) as well as the isotherm parameters (IP) obtained after fitting the experimental data to the equilibrium model, eq 2. The adjustment was made following several assumptions: (i) the pressure and gas velocity being constant, (ii) the bed porosity being uniform, (iii) a plug flow pattern without the effect of axial and radial dispersion, and (iv) a constant temperature.

RESULTS AND DISCUSSION

Prior to the CO_2 capture experiments, the synthesis and characterization of the C_{cap} were conducted. C_{cap} exhibited a regular spherical shape with a wall thickness of about 150 nm (Figure 1A) and a mean average diameter of around 900 nm (Figure 1B) as can be checked in the images of transmission and scanning microscopy. The carbon composition was 91.3% in weight (measured by EA), and the adsorption−desorption isotherms of N_2 at 77 K used to analyze their porous structure showed an A_{BET} of 1662 m^2/g with micropore and mesopore contributions (Figure S1 of the Supporting Information). Based on elemental analysis measurements, the prepared ENIL materials contain an IL mass percentage in the range of ∼60−74 wt % (Table 1). Those measurements were confirmed by the percentage of N, as established in a previous work.[33] The A_{BET} of the ENIL materials prepared was reduced till values of <5 m^2/g, demonstrating total porous coverage with the IL. The thermal stability of the ENIL materials is of special interest for gaseous applications, specifically in the regeneration stage, where high temperatures could be required. Although the decomposition temperature of a neat IL is generally above the process temperature, the IL−solid surface interaction when it is encapsulated may lead to a reduction in the thermal stability.[38]

https://doi.org/10.1021/acssuschemeng.2c02504
ACS Sustainable Chem. Eng. 2022, 10, 13917−13926

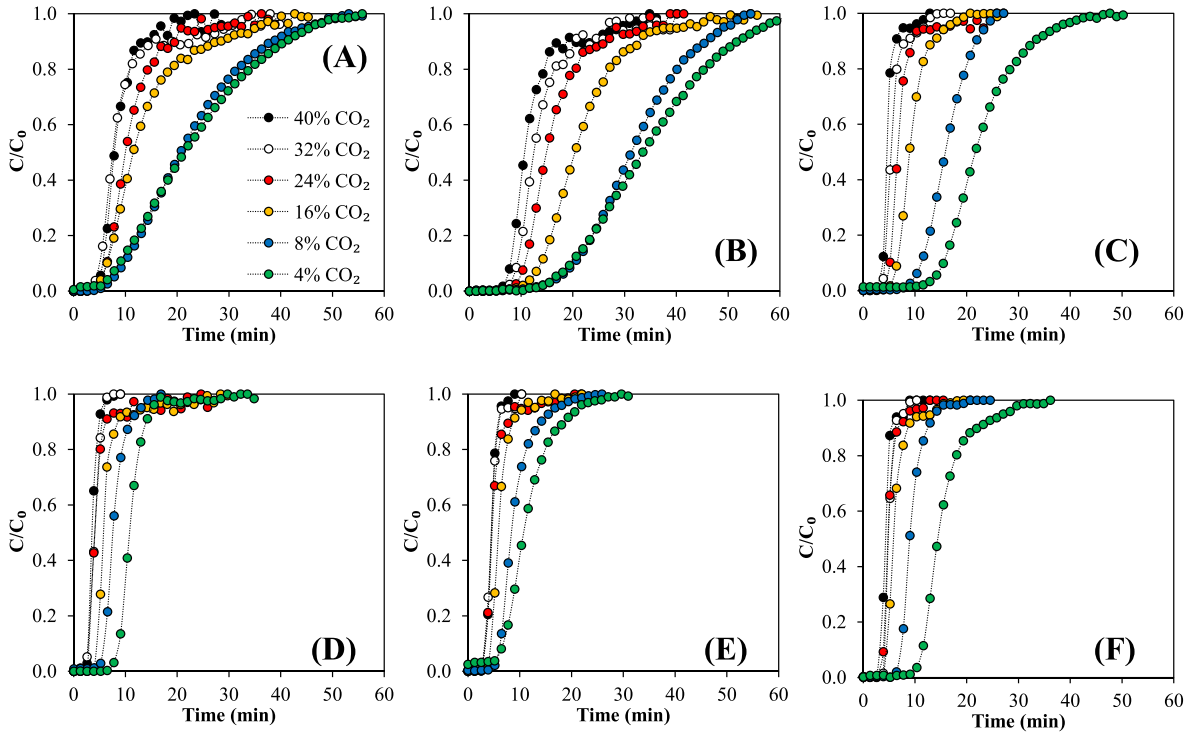

Figure 3. Breakthrough curves at different CO_2 partial pressures and 303 K for ENIL materials prepared from (A) [Emim][Acetate], (B) [Bmim][Acetate], (C) $[P_{66614}]$[CNPyr], (D) [Bmim][GLY], (E) [Bmim][MET], and (F) [Bmim][PRO].

The thermal stability of ENIL materials was examined by TGA in the range of 298 to 923 K. The TGA curves of Figure 2A−F show several pieces of evidence. First, ENIL materials present some sorbed water (less than 5% in weight), which needs to be removed in the degasification stage prior to CO_2 capture experiments. The hygroscopic characteristics of these ILs, especially aa-ILs, were previously reported.[42] The thermal stabilities of these ENIL materials are quite similar, starting to decompose at about 470 K, and at 600 K, the IL is practically degraded. These values can be compared with those of typical ILs designed for CO_2 chemical absorption. In deeper details, [Emim][Acetate] and [Bmim][Acetate] present a decomposition temperature of almost 500 K (Figure 2A,B),[21] clearly lower than the amino acid-based ILs (around 520 K).[27] If we compare them with $[P_{66614}]$[CNPyr], then the decomposition temperature is 550 K[24] due to the higher thermal stability of the phosphonium cation.

Moreover, considering the very low decomposition of the C_{Cap} support in this temperature range (stable until 1123 K, Figure S2 of the Supporting Information), the mass loss of ENIL in TGA curves is mainly attributed to IL degradation. As can be seen in Table 1, good agreement is found between the % IL measured by EA and TGA. Thus, the ENIL is confirmed as thermally stable under the CO_2 capture and regeneration conditions used in this study (333 K). Figure 2 also reports the derivative of the TGA curve, DTA of six ENIL materials, showing three peaks (dashed line), assigned to water (<373 K), subsequently the anion (~500 K), and finally the cation $[Bmim]^+$ (~510 K) or $[P_{66614}]^+$ (559 K).[44,45]

Figure 3 depicts the breakthrough curves obtained for the capture of CO_2 in streams composed by different $CO_2/CH_4/N_2$ concentrations at 303 K, using six different ILs with CO_2 chemical absorption. The estimated equilibrium CO_2 sorption capacity in mass of CO_2 (q_e) and moles of CO_2 (W_{CO_2}) per kg of ENIL sorbents were collected and are shown in Table 2. For comparison purposes, the thermodynamic (equilibrium) behavior of ENIL in CO_2 capture was also tested by gravimetric measurements, to complement the fixed-bed experiments. The CO_2 chemical absorption isotherms were obtained for six ENIL materials from 0.3 to 1 bar CO_2 partial pressures and from 0.04 to 0.4 bar according to the fixed-bed results (Figure 4) at 303 K. The Langmuir−Freundlich model was used to fit the experimental data. These comparisons let us validate both methodologies. As expected, the saturation CO_2 capacity increases with the CO_2 partial pressure, but great differences were observed depending on the nature of the IL used in the ENIL material. Acetate-based ENIL materials present the highest CO_2 sorption capacity, with the ENIL based on [Bmim][Acetate] being the one with the best CO_2 capture performance. The $[P_{66614}]$[CNPyr]-based ENIL presents a similar high CO_2 sorption capacity to the [Emim][Acetate]-based ENIL, whereas those ENIL materials derived from amino acids present a lower CO_2 solubility than the rest. As can be seen in Table 2, the CO_2 sorption capacity of ENIL sorbents matches the trend of CO_2 solubility in neat ILs, demonstrating that the efficiency of gas capture in a fixed bed using ENIL sorbents is determined by absorption thermodynamics rather than kinetics, in good agreement with a previous study.[17] Analyzing the role of the IL nature in Table 2 (Figure S3 of the Supporting Information), it can be checked that acetate-based ILs present the highest CO_2 capture, achieving solubilities of 1.18 and 0.88 mol/kg_{IL} for, respectively, [Bmim][Acetate] and [Emim][Acetate] cases followed by $[P_{66614}]$[CNPyr] (CO_2 solubility of 0.80 mol/kg_{IL}) and finally those derived from amino acids, which showed a CO_2 solubility of around 0.4 mol/kg_{IL} at a 0.4 bar CO_2 partial pressure and 303 K, in good agreement with previous absorption results.[21,46]

https://doi.org/10.1021/acssuschemeng.2c02504
ACS Sustainable Chem. Eng. 2022, 10, 13917−13926

Table 2. Operating Conditions and Results of the Fixed-Bed CO_2 Sorption Experiments at 303 K with the ENIL Materials Prepared

ENIL	p_{CO_2} (bar)	q_e($g \cdot kg_{ENIL}^{-1}$)	W_{CO_2}($mol \cdot kg_{ENIL}^{-1}$)	W_{CO_2}($mol \cdot kg_{IL}^{-1}$)	k_{YN} (min^{-1})	k_{MTC} (min^{-1})	H_{MTZ} (cm)	S_{CO_2/CH_4}
[Emim][Acetate]	0.04	6.33	0.14	0.22	0.16	0.19	4.5	1609
	0.08	12.30	0.28	0.44	0.17	0.22	4.5	
	0.16	15.60	0.35	0.55	0.31	0.29	4.4	
	0.24	19.29	0.44	0.69	0.39	0.41	4.4	
	0.32	21.77	0.49	0.77	0.59	0.48	4.2	
	0.40	24.88	0.57	0.88	0.76	0.56	4.3	
[Bmim][Acetate]	0.04	8.83	0.20	0.30	0.18	0.20	3.8	1343
	0.08	13.09	0.30	0.44	0.22	0.25	3.9	
	0.16	20.86	0.47	0.71	0.35	0.28	3.9	
	0.24	27.73	0.63	0.94	0.37	0.34	3.8	
	0.32	31.82	0.72	1.08	0.44	0.38	3.8	
	0.40	34.84	0.79	1.18	0.54	0.40	3.8	
[P_{66614}][CNPyr]	0.04	11.10	0.25	0.37	0.31	0.23	3.2	1362
	0.08	15.63	0.36	0.52	0.51	0.41	3.1	
	0.16	18.55	0.42	0.62	0.90	0.47	2.8	
	0.24	21.95	0.50	0.73	1.14	0.61	3.0	
	0.32	22.74	0.52	0.76	1.30	0.68	2.9	
	0.40	23.87	0.54	0.80	1.51	0.96	2.6	
[Bmim][GLY]	0.04	3.20	0.07	0.12	0.50	1.25	2.9	1555
	0.08	4.52	0.10	0.17	0.74	1.31	2.9	
	0.16	5.71	0.13	0.22	0.77	1.41	2.5	
	0.24	8.64	0.20	0.33	1.22	1.49	2.6	
	0.32	9.18	0.21	0.35	1.79	1.90	2.6	
	0.40	10.50	0.24	0.40	1.84	1.94	2.7	
[Bmim][PRO]	0.04	4.41	0.10	0.13	0.53	0.73	2.7	1701
	0.08	5.35	0.12	0.16	0.87	1.10	2.5	
	0.16	7.28	0.17	0.22	1.05	1.29	2.1	
	0.24	8.76	0.20	0.27	1.33	1.63	3.0	
	0.32	11.49	0.26	0.35	1.67	1.93	2.3	
	0.40	12.50	0.28	0.38	2.20	1.98	3.2	
[Bmim][MET]	0.04	3.05	0.07	0.10	0.37	0.65	3.8	1663
	0.08	4.91	0.11	0.16	0.59	0.97	3.6	
	0.16	6.81	0.15	0.23	1.00	1.11	3.4	
	0.24	8.49	0.19	0.28	1.23	1.35	3.2	
	0.32	9.82	0.22	0.33	1.68	1.82	3.0	
	0.40	12.08	0.27	0.40	1.82	1.98	3.0	

The main consideration is the practically negligible amount of CH_4 retained by the different ENIL materials (Figure S4 of the Supporting Information), which is below the equipment sensibility ($\sim 10^{-3}$ mol/kg). Therefore, the gas capture obtained for the six ENIL materials tested was mainly due to the chemical absorption of CO_2 by the IL, showing a remarkably high CO_2/CH_4 selectivity (>1000 for all ENIL studied, as can be seen in Table 2). Compared with the behavior of zeolites[47] and activated carbon[48,49] in the adsorption of CO_2/CH_4 mixtures, it can be clearly confirmed that ENIL materials showed a much higher selectivity to CO_2 than a wide range of supports. Attending to the adsorption capacity, some of the activated carbons with task-specific functionalization presented a higher CO_2 capacity (5.9 mol/kg at 303 K and 23 bar) but working at a high pressure and losing power selectivity to CO_2 (CO_2 selectivity of 4.7).[49] On the other hand, current results with ENIL sorbents improve those recently obtained with supported IL sorbents,[9,34,42] which may be related to the higher amount of IL incorporated into the ENIL material.

Once the thermodynamics of CO_2 capture is analyzed in a fixed bed using ENIL sorbents, the rate of CO_2 sorption is evaluated by fitting the experimental breakthrough curves to the kinetic models described in the Experimental Section. Table 2 collects the obtained characteristic kinetic parameters k_{YN} (Yoon and Nelson model, eq 3) and k_{MTC} (lumped resistance linear model, eq 6). Both kinetic models describe adequately the breakthrough curve slopes ($R^2 > 0.98$) over the whole range of solute concentrations studied for all the ENIL materials prepared. The estimated k_{YN} values (parameters in Table 2) vary in a wide range, from 0.16 to 0.76 min^{-1} for acetate based-ENIL materials to 0.37−2.20 min^{-1} for amino acid-based ENIL materials. Similarly, estimated k_{MTC} values indicate a wide range of CO_2 sorption kinetics depending on the CO_2 partial pressure and the type of ENIL used.

Figure 5A compares the k_{YN} values obtained from the experimental breakthrough curves for each ENIL at 303 K and different p_{CO_2}. As can be seen, the k_{YN} values show a nearly linear relationship with CO_2 partial pressure, which is related to the increasing solute concentration attending to eq 4. In order to evaluate the sorption rates of ENIL prepared using ILs with different CO_2 chemical absorption mass capacities (q_e in Table 2), Figure 5B compares the average k values (kg_{ENIL}^{-1}), which is a constant of proportionality obtained from eq 4,

https://doi.org/10.1021/acssuschemeng.2c02504
ACS Sustainable Chem. Eng. 2022, 10, 13917−13926

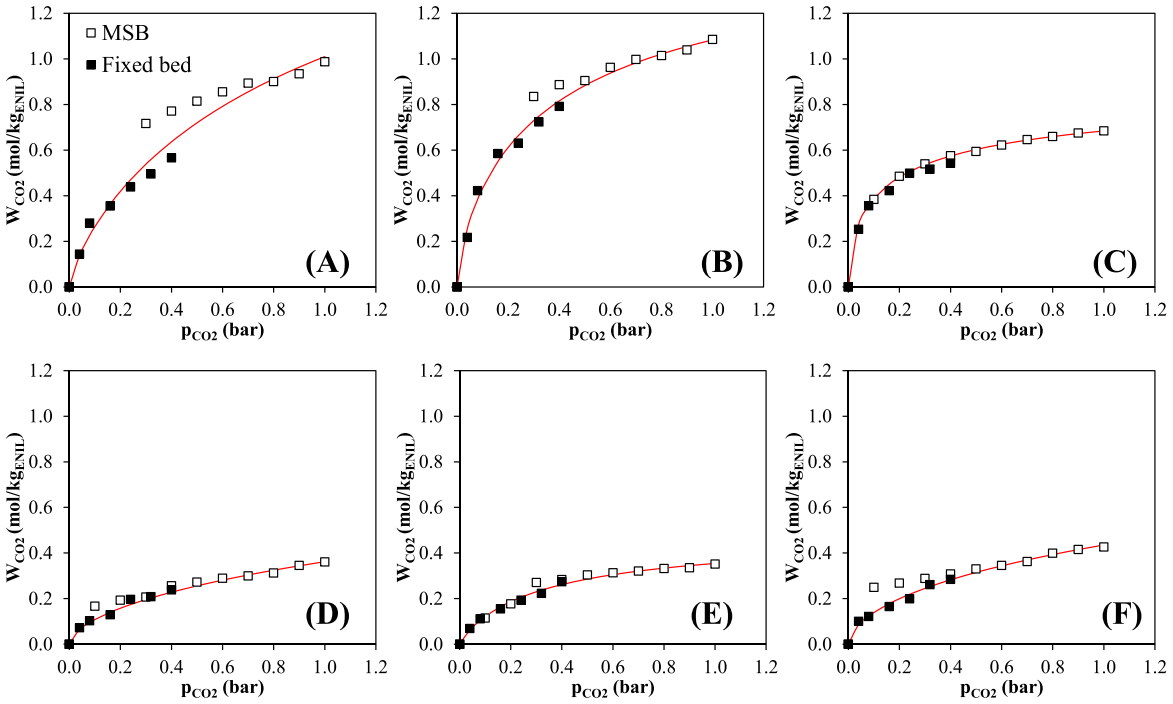

Figure 4. CO_2 isotherms of ENIL based on (A) [Emim][Acetate], (B) [Bmim][Acetate], (C) [P_{66614}][CNPyr], (D) [Bmim][GLY], (E) [Bmim][MET], and (F) [Bmim][PRO] at 303 K and different CO_2 partial pressures. The red line corresponds to the proposed chemical capture model and squares to experimental data (black squares were obtained by the fixed-bed column and white squares by the MSB).

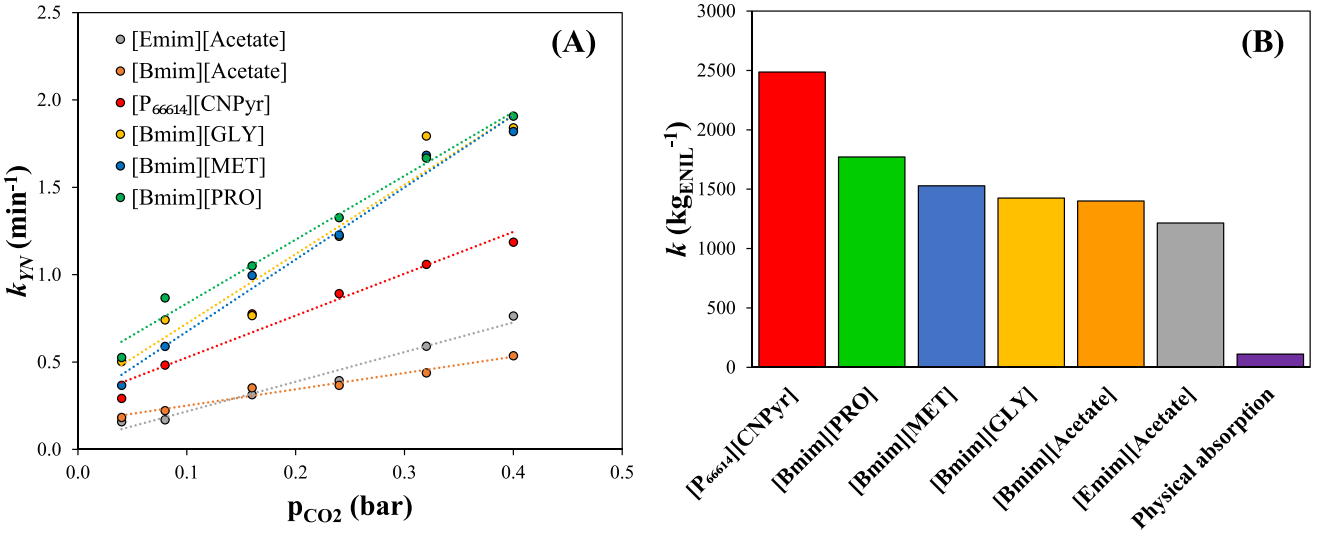

Figure 5. (A) k_{YN} (min^{-1}) kinetic constant at different CO_2 partial pressures obtained from fixed-bed experiments at 303 K using ~2−4 g of ENIL material and (B) average k values (kg$_{ENIL}^{-1}$) of eq 4, including the k data calculated with ENIL presenting CO_2 physical absorption for comparison purposes.

which eliminates the thermodynamic considerations of k_{YN}, for fixed-bed experiments (similar k values were obtained for different CO_2 partial pressures, Figure S5 of the Supporting Information). Figure 5B also includes the average k values previously obtained with ENIL presenting CO_2 physical absorption (at 10% CO_2 and 100 mLN/min).[17] It is concluded that ENIL sorbents with CO_2 chemical absorption present a significantly higher CO_2 capture rate than those with physical absorption. Regarding the different ENIL materials tested in this work, similar high sorption rates are obtained for acetate- and amino acid-based ILs (with k values in the range of around 1500 kg$_{ENIL}^{-1}$), suggesting that the CO_2 chemical capture rate is more influenced by the capsule morphology than by the IL nature, in good agreement with results obtained in CO_2 physical capture with ENIL.[17] The best results were obtained for AHA-IL [P_{66614}][CNPyr], probably due to the relatively low viscosity of IL reaction media[50] and the fast reaction kinetics.[28,29]

In a previous work,[34] the breakthrough curves of CO_2 capture in a fixed bed using [Bmim][Acetate] as the SILP sorbent were well-described by the LDF model represented by eq 6, obtaining an empirical equation to describe the increasing of the k_{MTC} kinetic coefficient when decreasing the sorbent particle size and increasing the CO_2 partial pressure. Figure 6A

https://doi.org/10.1021/acssuschemeng.2c02504
ACS Sustainable Chem. Eng. 2022, 10, 13917−13926

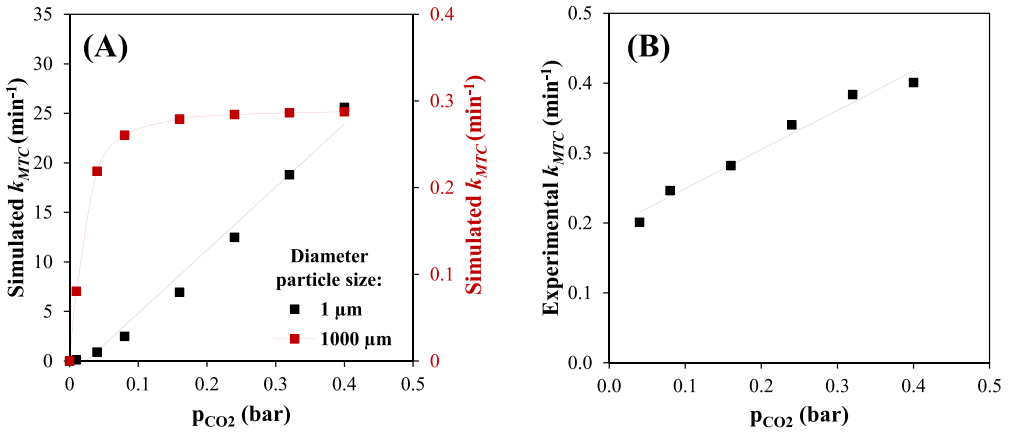

Figure 6. (A) k_{MTC} constant for CO_2 capture in a fixed bed using a simulated SILP material with [Bmim][Acetate] applying the empirical equation (eq 6) reported in ref 34 for two diameter particle sizes at different partial pressures and (B) experimental k_{MTC} (min^{-1}) kinetic constant for [Bmim][Acetate]-based ENIL at different CO_2 partial pressures obtained from fixed-bed experiments at 303 K.

shows the estimated k_{MTC} using such an empirical equation for a supported IL (using [Bmim][Acetate]) sorbent with two remarkably different particle sizes of 1000 (i.e., 1 mm, a common size for particle adsorbents) and 1 μm (value close to the ENIL size) at different CO_2 partial pressures. With a smaller particle size (1 μm), the kinetics of the CO_2 capture process is faster than found using sorbents with a higher particle diameter (1000 μm), consistent with the higher gas−liquid contact surface. In addition, the increase in the p_{CO_2} presents a remarkably different effect on the sorption rate when decreasing the sorbent particle size because of the shift of the control regime from CO_2 diffusion in the IL to the chemical absorption rate.[34] Figure 6B presents the experimental k_{MTC} values obtained in this work for the [Bmim][Acetate]-based ENIL (Table 2 collects the estimated k_{MTC} values for the rest of the ENIL sorbents prepared in this work) by fitting experimental breakthrough curves to the LDF model. A linear relationship is observed between the experimental and CO_2 partial pressures, in good agreement with simulated k_{MTC} (Figure 6A), which suggests that the CO_2 capture rate in ENIL using a fixed bed is determined by the reaction kinetics, overcoming the mass transfer control present in IL sorbents with a higher particle size.

Table 2 includes the estimated height of the mass transfer zone (H_{MTZ}, eq 5), calculated from each breakthrough curve as an additional parameter of the performance of ENIL sorbents in a fixed bed for a CO_2 capture system. H_{MTZ} values are in a narrow range from 3 to 4.5 cm (also depending on the fixed-bed height), in good agreement with previous results for CO_2 chemical capture with ENIL[21] and slightly lower than those obtained with ENIL materials prepared with ILs that provide CO_2 capture by physical absorption[17] and H_{MTZ} values obtained in CO_2 fixed-bed capture using conventional solid sorbents.[40] These results reveal fast and favorable CO_2 chemical sorption into ENIL materials in fixed-bed operation, ascribable to the high sorption capacity (high amount of ILs incorporated in the ENIL) and CO_2/CH_4 selectivity, together with the large gas−liquid contact area and the small particle size, which overcomes the mass transfer limitations of ILs and promotes a fast CO_2 sorption process governed by the chemical reaction kinetics, maximizing the efficient use of ENIL sorbents in the fixed-bed process.

CONCLUSIONS

In this work, encapsulated ionic liquid materials (ENIL) were specifically prepared for CO_2 capture from $CO_2/CH_4/N_2$ effluents, and their performance was evaluated by means of gravimetric and fixed-bed measurements. The first step was the preparation of ENIL materials, with around 70% in mass of IL inside them, to be used as the sorbent material. Six ILs based on acetate, amino acid, and aprotic heterocyclic anion presenting CO_2 chemical absorption were selected to increase the CO_2 uptake and CO_2/CH_4 selectivity of ENIL materials. Fixed-bed and gravimetric measurements revealed that all the ENIL materials showed high CO_2 sorption capacity and negligible CH_4 capture, obtaining very favorable thermodynamic performance for CO_2/CH_4 separation. All the experimental breakthrough curves were successfully fitted to Yoon and Nelson and LDF models. The kinetic analysis revealed that ENIL sorbents also present a remarkably favorable CO_2 capture rate due to the small capsule size and, correspondingly, the high gas−liquid contact surface, which overcomes the mass transfer limitations of ILs and seems to promote CO_2 capture in a fixed bed controlled by the reaction kinetics. Current results present ENIL as advanced sorbents with exceptional CO_2/CH_4 gas separation performance in fixed-bed technology, obtaining [P_{66614}][CNPyrr]-based ENIL as the most promising material due to both favorable kinetic and thermodynamic properties.

ASSOCIATED CONTENT

Supporting Information

The Supporting Information is available free of charge at https://pubs.acs.org/doi/10.1021/acssuschemeng.2c02504.

Kinetic parameters of the LDF model, N_2 adsorption isotherm at 77 K of carbon capsules, thermogravimetric analysis of carbon capsules, CO_2 isotherms of ENIL, CH_4 isotherms of ENIL, and k proportionality constant for CO_2 capture in a fixed bed using ENIL (PDF)

AUTHOR INFORMATION

Corresponding Author

J. Lemus − *Chemical Engineering Department, Universidad Autónoma de Madrid, 28049 Madrid, Spain;* orcid.org/0000-0001-5386-2868; Email: jesus.lemus@uam.es

https://doi.org/10.1021/acssuschemeng.2c02504
ACS Sustainable Chem. Eng. 2022, 10, 13917−13926

Authors

C. Paramio − *Chemical Engineering Department, Universidad Autónoma de Madrid, 28049 Madrid, Spain*

D. Hospital-Benito − *Chemical Engineering Department, Universidad Autónoma de Madrid, 28049 Madrid, Spain*

C. Moya − *Chemical Engineering Department, Universidad Autónoma de Madrid, 28049 Madrid, Spain;* orcid.org/0000-0001-5107-7751

R. Santiago − *Chemical Engineering Department, Universidad Autónoma de Madrid, 28049 Madrid, Spain;* orcid.org/0000-0002-6877-9001

J. Palomar − *Chemical Engineering Department, Universidad Autónoma de Madrid, 28049 Madrid, Spain;* orcid.org/0000-0003-4304-0515

Complete contact information is available at: https://pubs.acs.org/10.1021/acssuschemeng.2c02504

Notes

The authors declare no competing financial interest.

■ ACKNOWLEDGMENTS

The authors are grateful to Ministerio de Ciencia e Innovación of Spain (projects PID2020-118259RB-I00 and PDC2021-120881-I00) and Comunidad de Madrid (project P2018/EMT4348) for financial support and Centro de Computación Científica de la Universidad Autónoma de Madrid for computational facilities.

■ REFERENCES

(1) Grignard, B.; Gennen, S.; Jérôme, C.; Kleij, A. W.; Detrembleur, C. Advances in the use of CO_2 as a renewable feedstock for the synthesis of polymers. *Chem. Soc. Rev.* **2019**, *48*, 4466−4514.

(2) Zhou, K.; Chaemchuen, S.; Verpoort, F. Alternative materials in technologies for Biogas upgrading via CO_2 capture. *Renewable Sustainable Energy Rev.* **2017**, *79*, 1414−1441.

(3) Adnan, A. I.; Ong, M. Y.; Nomanbhay, S.; Chew, K. W.; Show, P. L. Technologies for Biogas Upgrading to Biomethane: A Review. *Bioengineering* **2019**, *6*, 92.

(4) Mondal, M. K.; Balsora, H. K.; Varshney, P. Progress and trends in CO_2 capture/separation technologies: A review. *Energy* **2012**, *46*, 431−441.

(5) Ferella, F.; Puca, A.; Taglieri, G.; Rossi, L.; Gallucci, K. Separation of carbon dioxide for biogas upgrading to biomethane. *J. Cleaner Prod.* **2017**, *164*, 1205−1218.

(6) Osman, A. I.; Hefny, M.; Abdel Maksoud, M. I. A.; Elgarahy, A. M.; Rooney, D. W. Recent advances in carbon capture storage and utilisation technologies: a review. *Environ. Chem. Lett.* **2021**, *19*, 797−849.

(7) Karacan, C. Ö.; Ruiz, F. A.; Cotè, M.; Phipps, S. Coal mine methane: A review of capture and utilization practices with benefits to mining safety and to greenhouse gas reduction. *Int. J. Coal Geol.* **2011**, *86*, 121−156.

(8) Wang, L.; Xie, H.; Huang, X.; Xu, Y.; Chu, T.; Wu, Z. CO_2 and CH_4 Sorption by Solid-State Ammonium and Imidazolium Ionic Liquids. *Energy Fuels* **2020**, *35*, 599−609.

(9) Durak, O.; Zeeshan, M.; Keskin, S.; Uzun, A. [BMIM][OAc] coating layer makes activated carbon almost completely selective for CO_2. *Chem. Eng. J.* **2022**, *437*, 135436.

(10) Kapoor, R.; Ghosh, P.; Kumar, M.; Vijay, V. K. Evaluation of biogas upgrading technologies and future perspectives: a review. *Environ. Sci. Pollut Res.. Int.* **2019**, *26*, 11631−11661.

(11) Reddy, S.; Yonkoski, J.; Rode, H.; Irons, R.; Albrecht, W. Fluor's Econamine FG PlusSM Completes Test Program at Uniper's Wilhelmshaven Coal Power Plant. *Energy Procedia* **2017**, *114*, 5816−5825.

(12) Nakamura, S.; Yamanaka, Y.; Matsuyama, T.; Okuno, S.; Sato, H.; Iso, Y.; Huang, J. Effect of Combinations of Novel Amine Solvents, Processes and Packing at IHI's Aioi Pilot Plant. *Energy Procedia* **2014**, *63*, 687−692.

(13) Kim, J.; Na, J.; Kim, K.; Bak, J. H.; Lee, H.; Lee, U. Learning the properties of a water-lean amine solvent from carbon capture pilot experiments. *Appl. Energy* **2021**, *283*, 116213.

(14) Lei, Z.; Dai, C.; Chen, B. Gas Solubility in Ionic Liquids. *Chem. Rev.* **2014**, *114*, 1289−1326.

(15) Shukla, S. K.; Khokarale, S. G.; Bui, T. Q.; Mikkola, J.-P. T. Ionic Liquids: Potential Materials for Carbon Dioxide Capture and Utilization. *Front. Mater.* **2019**, *6*, 42.

(16) Palomar, J.; Larriba, M.; Lemus, J.; Moreno, D.; Santiago, R.; Moya, C.; de Riva, J.; Pedrosa, G. Demonstrating the key role of kinetics over thermodynamics in the selection of ionic liquids for CO_2 physical absorption. *Sep. Purif. Technol.* **2019**, *213*, 578−586.

(17) Santiago, R.; Lemus, J.; Moreno, D.; Moya, C.; Larriba, M.; Alonso-Morales, N.; Gilarranz, M. A.; Rodríguez, J. J.; Palomar, J. From kinetics to equilibrium control in CO_2 capture columns using Encapsulated Ionic Liquids (ENILs). *Chem. Eng. J.* **2018**, *348*, 661−668.

(18) Carvalho, P. J.; Kurnia, K. A.; Coutinho, J. A. Dispelling some myths about the CO_2 solubility in ionic liquids. *Phys. Chem. Chem. Phys.* **2016**, *18*, 14757−14771.

(19) Gurau, G.; Rodriguez, H.; Kelley, S. P.; Janiczek, P.; Kalb, R. S.; Rogers, R. D. Demonstration of Chemisorption of Carbon Dioxide in 1,3-Dialkylimidazolium Acetate Ionic Liquids. *Angew. Chem.* **2011**, *50*, 12024−12026.

(20) Cabaco, M. I.; Besnard, M.; Danten, Y.; Coutinho, J. A. P. Carbon Dioxide in 1-Butyl-3-methylimidazolium Acetate, I. Unusual Solubility Investigated by Raman Spectroscopy and DFT Calculations. *J. Phys. Chem. A* **2012**, *116*, 1605−1620.

(21) Moya, C.; Alonso-Morales, N.; Gilarranz, M. A.; Rodriguez, J. J.; Palomar, J. Encapsulated Ionic Liquids for CO_2 Capture: Using 1-Butyl-methylimidazolium Acetate for Quick and Reversible CO_2 Chemical Absorption. *ChemPhysChem* **2016**, *17*, 3891−3899.

(22) Gurkan, B.; Goodrich, B. F.; Mindrup, E. M.; Ficke, L. E.; Massel, M.; Seo, S.; Senftle, T. P.; Wu, H.; Glaser, M. F.; Shah, J. K.; Maginn, E. J.; Brennecke, J. F.; Schneider, W. F. Molecular Design of High Capacity, Low Viscosity, Chemically Tunable Ionic Liquids for CO_2 Capture. *J. Phys. Chem. Lett.* **2010**, *1*, 3494−3499.

(23) Seo, S.; Quiroz-Guzman, M.; DeSilva, M. A.; Lee, T. B.; Huang, Y.; Goodrich, B. F.; Schneider, W. F.; Brennecke, J. F. Chemically Tunable Ionic Liquids with Aprotic Heterocyclic Anion (AHA) for CO_2 Capture. *J. Phys. Chem. B* **2014**, *118*, 5740−5751.

(24) Moya, C.; Alonso-Morales, N.; de Riva, J.; Morales-Collazo, O.; Brennecke, J. F.; Palomar, J. Encapsulation of Ionic Liquids with an Aprotic Heterocyclic Anion (AHA-IL) for CO_2 Capture: Preserving the Favorable Thermodynamics and Enhancing the Kinetics of Absorption. *J. Phys. Chem. B* **2018**, *122*, 2616−2626.

(25) Zhang, J.; Zhang, S. J.; Dong, K.; Zhang, Y.; Shen, Y.; Lv, X. Supported absorption of CO_2 by tetrabutylphosphonium amino acid ionic liquids. *Chem. - Eur. J.* **2006**, *12*, 4021−4026.

(26) Chen, F. F.; Huang, K.; Zhou, Y.; Tian, Z. Q.; Zhu, X.; Tao, D. J.; Jiang, D. E.; Dai, S. Multi-Molar Absorption of CO_2 by the Activation of Carboxylate Groups in Amino Acid Ionic Liquids. *Angew. Chem.* **2016**, *55*, 7166−7170.

(27) Santiago, R.; Lemus, J.; Moya, C.; Moreno, D.; Alonso-Morales, N.; Palomar, J. Encapsulated Ionic Liquids to Enable the Practical Application of Amino Acid-Based Ionic Liquids in CO_2 Capture. *ACS Sustainable Chem. Eng.* **2018**, *6*, 14178.

(28) Hospital-Benito, D.; Lemus, J.; Moya, C.; Santiago, R.; Ferro, V. R.; Palomar, J. Techno-economic feasibility of ionic liquids-based CO_2 chemical capture processes. *Chem. Eng. J.* **2021**, *407*, 127196.

(29) Hospital-Benito, D.; Lemus, J.; Moya, C.; Santiago, R.; Palomar, J. Process analysis overview of ionic liquids on CO_2 chemical capture. *Chem. Eng. J.* **2020**, *390*, 124509.

(30) Angelidaki, I.; Treu, L.; Tsapekos, P.; Luo, G.; Campanaro, S.; Wenzel, H.; Kougias, P. G. Biogas upgrading and utilization: Current status and perspectives. *Biotechnol. Adv.* **2018**, *36*, 452−466.
(31) Yan, J.; Mangolini, F. Engineering encapsulated ionic liquids for next-generation applications. *RSC Adv.* **2021**, *11*, 36273−36288.
(32) Lemus, J.; Bedia, J.; Moya, C.; Alonso-Morales, N.; Gilarranz, M. A.; Palomar, J.; Rodriguez, J. J. Ammonia capture from the gas phase by encapsulated ionic liquids (ENILs). *RSC Adv.* **2016**, *6*, 61650−61660.
(33) Palomar, J.; Lemus, J.; Alonso-Morales, N.; Bedia, J.; Gilarranz, M. A.; Rodriguez, J. J. Encapsulated ionic liquids (ENILs): from continuous to discrete liquid phase. *Chem. Commun.* **2012**, *48*, 10046−10048.
(34) Santiago, R.; Lemus, J.; Hospital-Benito, D.; Moya, C.; Bedia, J.; Alonso-Morales, N.; Rodriguez, J. J.; Palomar, J. CO_2 Capture by Supported Ionic Liquid Phase: Highlighting the Role of the Particle Size. *ACS Sustainable Chem. Eng.* **2019**, *7*, 13089−13097.
(35) Lemus, J.; Da Silva, F. F. A.; Palomar, J.; Carvalho, P. J.; Coutinho, J. A. P. Solubility of carbon dioxide in encapsulated ionic liquids. *Sep. Purif. Technol.* **2018**, *196*, 41−46.
(36) Alonso-Morales, N.; Gilarranz, M. A.; Palomar, J.; Lemus, J.; Heras, F.; Rodriguez, J. J. Preparation of hollow submicrocapsules with a mesoporous carbon shell. *Carbon* **2013**, *59*, 430−438.
(37) Stöber, W.; Fink, A.; Bohn, E. Controlled Growth of Monodisperse Silica Spheres in the Micron Size Range. *J. Colloid Interface Sci.* **1968**, *26*, 62−69.
(38) Lemus, J.; Palomar, J.; Gilarranz, M. A.; Rodriguez, J. J. Characterization of Supported Ionic Liquid Phase (SILP) materials prepared from different supports. *Adsorption* **2011**, *17*, 561−571.
(39) Yoon, Y. H.; Nelson, J. H. Breakthrough time and adsorption capacity of respirator cartridges. *Am. Ind. Hyg. Assoc. J.* **1992**, *53*, 303−316.
(40) Lemus, J.; Martin-Martinez, M.; Palomar, J.; Gomez-Sainero, L.; Gilarranz, M. A.; Rodriguez, J. J. Removal of chlorinated organic volatile compounds by gas phase adsorption with activated carbon. *Chem. Eng. J.* **2012**, *211-212*, 246−254.
(41) Yoon, Y. H.; Nelson, J. H. Application of Gas Adsorption Kinetics — II. A Theoretical Model for Respirator Cartridge Service Life and Its Practical Applications. *Am. Ind. Hyg. Assoc. J.* **1984**, *45*, 517−524.
(42) Balsamo, M.; Erto, A.; Lancia, A.; Totarella, G.; Montagnaro, F.; Turco, R. Post-combustion CO_2 capture: On the potentiality of amino acid ionic liquid as modifying agent of mesoporous solids. *Fuel* **2018**, *218*, 155−161.
(43) Quijada-Maldonado, E.; van der Boogaart, S.; Lijbers, J. H.; Meindersma, G. W.; de Haan, A. B. Experimental densities, dynamic viscosities and surface tensions of the ionic liquids series 1-ethyl-3-methylimidazolium acetate and dicyanamide and their binary and ternary mixtures with water and ethanol at T=(298.15 to 343.15K). *J. Chem. Thermodyn.* **2012**, *51*, 51−58.
(44) Cao, Y.; Mu, T. Comprehensive Investigation on the Thermal Stability of 66 Ionic Liquids by Thermogravimetric Analysis. *Ind. Eng. Chem. Res.* **2014**, *53*, 8651−8664.
(45) Saeed, S.; Saleem, M.; Durrani, A. K. Thermal performance analysis of low-grade coal pretreated by ionic liquids possessing imidazolium, ammonium and phosphonium cations. *Fuel* **2020**, *271*, 117655.
(46) Zhao, M.; Wei, L.; Zheng, Y. K.; Liu, M. P.; Wang, J. L.; Qiu, Y. P. Structural effect of imidazolium-type ionic liquid adsorption to montmorillonite. *Sci. Total Environ.* **2019**, *666*, 858−864.
(47) Nguyen, H. G. T.; Sims, C. M.; Toman, B.; Horn, J.; van Zee, R. D.; Thommes, M.; Ahmad, R.; Denayer, J. F. M.; Baron, G. V.; Napolitano, E.; Bielewski, M.; Mangano, E.; Brandani, S.; Broom, D. P.; Benham, M. J.; Dailly, A.; Dreisbach, F.; Edubilli, S.; Gumma, S.; Möllmer, J.; Lange, M.; Tian, M.; Mays, T. J.; Shigeoka, T.; Yamakita, S.; Hakuman, M.; Nakada, Y.; Nakai, K.; Hwang, J.; Pini, R.; Jiang, H.; Ebner, A. D.; Nicholson, M. A.; Ritter, J. A.; Farrando-Pérez, J.; Cuadrado-Collados, C.; Silvestre-Albero, J.; Tampaxis, C.; Steriotis, T.; Řimnáčová, D.; Švábová, M.; Vorokhta, M.; Wang, H.; Bovens, E.; Heymans, N.; De Weireld, G. A reference high-pressure CH_4 adsorption isotherm for zeolite Y: results of an interlaboratory study. *Adsorption* **2020**, *26*, 1253−1266.
(48) Cleeton, C.; Farmahini, A. H.; Sarkisov, L. Performance-based ranking of porous materials for PSA carbon capture under the uncertainty of experimental data. *Chem. Eng. J.* **2022**, *437*, 135395.
(49) Peredo-Mancilla, D.; Ghimbeu, C. M.; Ho, B.-N.; Jeguirim, M.; Hort, C.; Bessieres, D. Comparative study of the CH_4/CO_2 adsorption selectivity of activated carbons for biogas upgrading. *J. Environ. Chem. Eng.* **2019**, *7*, 103368.
(50) Zhai, H.; Rubin, E. S. Systems Analysis of Ionic Liquids for Post-combustion CO_2 Capture at Coal-fired Power Plants. *Energy Procedia* **2014**, *63*, 1321−1328.